

The Hourglass Nebulae of Sher 25 and SN 1987 A: Two of a Kind?¹

Wolfgang Brandner^{2,3}, You-Hua Chu^{2,4}, Frank Eisenhauer⁵, Eva K. Grebel³, Sean D. Points²

²*University of Illinois at Urbana-Champaign, Department of Astronomy, 1002 West Green Street, Urbana, IL 61801, USA*

³*Astronomisches Institut der Universität Würzburg, Am Hubland, D-97074 Würzburg, Germany*

⁴*Visiting astronomer, Cerro Tololo Inter-American Observatory, NOAO, which are operated by AURA, Inc., under contract with the NSF*

⁵*Max-Planck-Institut für extraterrestrische Physik, Giessenbachstraße, D-85740 Garching, Germany*

ABSTRACT

We have performed a detailed study of the morphology and kinematics of the hourglass-shaped nebula around the blue supergiant Sher 25 in the galactic giant HII region NGC 3603. Near-infrared high resolution adaptive optics images in the Br γ line and HST/NICMOS images in the HeI 1.08 μ m line were compared with iso-velocity maps in the H α and [NII] lines.

The adaptive optics observations clearly resolved the width of the ring (0''.9, i.e., 0.027 pc), yielding $\delta R/R=1:8$. We show that the H α and [NII] lines trace the entire silhouette of the hourglass. The bipolar lobes of the hourglass expand at 70 km s⁻¹, whereas the ring around the waist of the hourglass expands at 30 km s⁻¹. Both the ring and the bipolar lobes have about the same dynamical age, indicating a common origin and a major outburst and mass-loss event 6630 yr ago. The ionized mass within the hourglass is between 0.3 M $_{\odot}$ and 0.6 M $_{\odot}$ - quite comparable to the total mass suggested for the expanding (pre-supernova) shell around SN 1987 A.

The hourglass structure around Sher 25 is similar to that of SN 1987 A in spatial extent, mass, and velocities. The major differences between these two nebulae might arise from environmental effects. Both internal and external ionization sources are available for Sher 25's nebula. Furthermore, Sher 25 and its hourglass-shaped nebula appear to be moving to the south-west with respect to the ambient interstellar medium, and ram pressure has apparently deformed the hourglass. We conclude that the circumstellar nebulae around SN 1987 A and Sher 25 are very similar and define a new class of nebulae around blue supergiants in their final evolutionary stage.

Subject headings: Stars: evolution, individual (Sher 25), mass-loss, and supergiants – supernovae: individual (SN 1987 A) – ISM: individual (NGC 3603).

¹Based on observations obtained at CTIO, at the European Southern Observatory, La Silla (ESO Proposal No. 58.E-0965, 59.D-0330), and on observations made with the NASA/ESA Hubble Space Telescope, obtained from the data archive at the Space Telescope Science Institute. STScI is operated by the Association of Universities for Research in Astronomy, Inc., under the NASA contract NAS 5-26555.

1. Introduction

The HII ring around Sher 25 was serendipitously discovered (Brandner et al. 1997) in the course of a high-spectral resolution study of emission line knots in the giant HII NGC 3603 region (distance 6 kpc, e.g., Clayton 1986). It has a diameter of 0.4 pc, is tilted by 65° against the plane of the sky, and is expanding. Perpendicular to the plane of the ring are two extended nebular structures which appear to be bipolar lobes. The high [NII]/H α ratio of 2.1:1 in the nebular material gives evidence that we see circumstellar material enriched by the CNO cycle and ejected by Sher 25 (Brandner et al. 1997).

The present study aims at investigating the physical structure and dynamics of the ring and bipolar outflow around Sher 25. Through a comparison to SN 1987A's rings we hope to gain a better understanding of the basic physics and formation mechanisms of bipolar nebulae around blue supergiants.

2. Observations and data reduction

Low-dispersion spectra of Sher 25's nebula were obtained on 1997 February 3 with the ESO/MPI 2.2m telescope and EFOSC2. The slit width was $1''.5$. The spectra have a resolution of $0.2 \text{ nm pixel}^{-1}$ and cover the wavelength range from 517 nm to 928 nm. They were wavelength and flux calibrated using IRAF².

Long-slit echelle spectroscopic mapping of Sher 25's nebula was carried out on 1997 February 27 at the CTIO 4m telescope. The cross disperser of the echelle spectrograph had been replaced by a flat mirror. To map Sher 25's nebula, we used an east-west oriented slit (slit width $1''.65$) and observed 14 slit positions, spaced by $2''$ from $12''$ north to $14''$ south of Sher 25. The integration time per slit position was 10 min and the velocity resolution $\approx 3.8 \text{ km s}^{-1} \text{ pixel}^{-1}$. The final spatial resolution in east-west direction, i.e. along the slit was $1''.7$ (seeing), and $4''$ in north-south direction. Using IRAF we flat-fielded, rectified, and wavelength calibrated the 2-D frames. They then were stacked into a 3-D data cube and analyzed with IDL.

Adaptive optics imaging of Sher 25 and its nebula was carried out with ADONIS/SHARP at the ESO 3.6m telescope on 1997 May 19. We observed with a Fabry-Perot-Etalon ($\lambda/\delta\lambda=2200$) centered on Br γ ($2.166\mu\text{m}$) and the nearby continuum ($2.157\mu\text{m}$ and

$2.174\mu\text{m}$). For both line and continuum we obtained $40 \times 1 \text{ min}$ exposures. Due to a very short coherence time of the atmospheric turbulence, the spatial resolution achieved was not diffraction limited but $0''.35$. The individual exposures were sky-subtracted, flat-fielded, aligned, and coadded.

The central cluster of NGC 3603 has been chosen for the initial focus alignment and the on-going focus monitoring (PI: G. Schneider, A. Suchkov) of the new NICMOS instrument at the Hubble Space Telescope. Because of its proximity to the central cluster, Sher 25 is included in all HST/NICMOS observations with camera 3 (NIC3) centered on the cluster. We retrieved 18 calibrated images in the HeI $1.08 \mu\text{m}$ line observed between May 6 and July 28 1997 from the HST archive. The total integration time was 608s. We rotated all images to a common orientation. Using our own IDL procedures, the individual images were then cross-correlated with each other in order to determine the offsets. Then the images were Fourier-shifted (to allow for the sub-pixel alignment) and coadded. Due to technical problems with NIC3, the images were slightly out of focus. The coadded image has a resolution of $0''.7$, whereas the best individual exposure had a resolution of $0''.5$.

3. Dynamical Structure of Sher25's Nebula

To study the morphology of the nebula in distinct velocity bins we extracted iso-velocity maps from the 3-D data cube. The maps clearly trace the expanding ring and the bipolar lobes. In Figure 1 (Plate x) we show iso-velocity maps in the [NII] 658.4 nm line (upper panel) and H α line (lower panel). The velocity offset between individual maps is 7.556 km s^{-1} . The zero point was chosen in such a way that the line of nodes of the ring has a velocity of 0 km s^{-1} . A non-uniform background arising from the giant HII region NGC 3603 is present in almost all of the H α maps.

The overall structure of Sher 25's nebula has the shape of an hourglass with the inner ring at the waist of the hourglass. The ring is clumpy and coplanar. It is most prominent in the velocity channels between -30.2 km s^{-1} and $+30.2 \text{ km s}^{-1}$. The bright bipolar lobes lie on the surface of the hourglass. Its silhouette can be traced on individual iso-velocity maps. The north-eastern silhouette is best visible in the velocity range of -22.7 km s^{-1} to -7.6 km s^{-1} , whereas the south-western silhouette is best visible in the velocity range of $+7.6 \text{ km s}^{-1}$ to $+22.7 \text{ km s}^{-1}$. Each

²IRAF is distributed by the National Optical Astronomy Observatories (NOAO)

of these bipolar lobes is pretty much complete. In addition, a compact, high-velocity “bullet” is present in each lobe. The bullet-type knots have velocities of up to $\pm 60.4 \text{ km s}^{-1}$. In some of the iso-velocity maps a faint linear structure seems to connect the south-western “bullet” with Sher 25 (most prominent from $+7.6 \text{ km s}^{-1}$ to $+30.2 \text{ km s}^{-1}$). Apart from these high-velocity components, the tips of the bipolar lobes are restricted to projected velocities of $\pm 30 \text{ km s}^{-1}$.

The two halves of the hourglass are asymmetric with respect to the plane of the ring. While both lobes extend to equal distances above and below the plane, their shapes are different. The north-eastern lobe is prolate and the south-western lobe is oblate with respect to the polar axis. The bipolar caps show a rather complex structure. The south-western polar cap is beret-shaped and is seen almost edge-on. The bright rims of the cap can be seen easily on $\text{H}\alpha$ images (cf. Brandner et al. 1997, Fig. 2/Plate L9). The beret shape might result from ram pressure as the whole nebula appears to be moving to the south-west relative to the interstellar medium (see below).

Assuming that all nebular material has been ejected by Sher 25 instantaneously, the radial velocity of the material is directly proportional to its distance from Sher 25 along the line of sight. Tomographic imaging techniques can then be applied to visualize the 3-D structure of the nebula. In Figure 2 we show the nebula as seen from different viewing angles (215° & 165°).

As can be seen from Figure 3, Sher 25 itself is displaced to the southwest with respect to the center of the inner ring. This and the asymmetry in the bipolar lobes indicate that Sher 25 and the whole outflow structure might be moving relative to the ambient interstellar medium. We confirm that the ring has an inclination angle of $\approx 65^\circ$ as derived by Brandner et al. (1997). The expansion velocities of the ring and the bipolar lobes, however, differ slightly from previous estimates. The discovery of the expanding ring and the velocity estimates were based on a single long-slit spectra across the north-eastern lobe and the ring (Brandner et al. 1997). Our new observations cover the entire hourglass nebula and yield a deprojected expansion velocity of 30 km s^{-1} for the ring. The bipolar lobes show deprojected velocities of 70 km s^{-1} , whereas the high-velocity knots are moving with velocities up to 140 km s^{-1} .

With these improved velocities, we derive a dynamical age of 6560 yr for the ring (diameter 0.4 pc),

and a dynamical age of 6700 yr for the bipolar lobes, which extend to about 0.7 pc above and below the plane of the ring. Thus, both the ring and the bipolar lobes can be traced back to the same mass ejection event, which occurred approximately 6630 yr ago (averaging the two ages). The high-velocity knots might be younger ($\approx 3400 \text{ yr}$).

4. Physical Properties of Sher 25’s Nebula

Figure 3 (Plate xx) shows emission line images of Sher 25’s ring in the $\text{H}\alpha$ (top), $\text{HeI } 1.08 \mu\text{m}$ (middle), and $\text{Br}\gamma$ (bottom) lines. The width of the ring, $0''.9$ (0.027 pc or $8 \times 10^{16} \text{ cm}$, i.e., $\delta R/R=1:8$), is clearly resolved in the near-infrared adaptive optics images in the $\text{Br}\gamma$ line and the HST/NICMOS images in the HeI line.

No temperature-sensitive line combinations were available in our spectra. We thus assumed a temperature of 10^4 K which is typical for HII regions. Electron densities were computed in two independent ways, based on the $\text{H}\alpha$ surface brightness and using the $[\text{SII}] 671.7 \text{ nm} / [\text{SII}] 673.1 \text{ nm}$ line ratios. Both calculations agreed within a factor of two. The electron density in the ring is around 10^3 cm^{-3} in the bright knots and drops to 500 cm^{-3} in the faint filaments between bright knots. Only the bright feature at the southern rim of the ring shows a higher electron density of $1.8 \times 10^3 \text{ cm}^{-3}$. In the brightest knot of the north-eastern lobe we measure an average electron density of around $1.5 \times 10^3 \text{ cm}^{-3}$, with a peak value of $3 \times 10^3 \text{ cm}^{-3}$. The south-western lobe has a mean electron density of $1.6 \times 10^3 \text{ cm}^{-3}$.

The masses deduced from the free electron densities depend strongly on the geometry of the nebular material. The adaptive optics image allows us to resolve the width of the ring. The beret-shaped polar cap at the top of the south-western lobe is resolved into two layers that correspond to the receding and approaching rim of the cap, respectively. The masses given in Table 1 assume a depth comparable to the minor axis (lower limit) or a depth comparable to the major axis (upper limit) for the knots. The total ionized mass in the ring and the lobes is $\leq 0.7 M_\odot$. Since this is small compared to the total mass loss of a massive star over its lifetime, and the dynamical age of the ring and the lobes are similar, we conclude that the mass ejection event occurred during a brief and violent phase with a very high mass-loss rate.

The smallest $[\text{NII}]/\text{H}\alpha$ ratio can be found in the

TABLE 1
ELECTRON DENSITY, MASS, AND VELOCITY IN THE RING AND OUTFLOWS AROUND SHER25.

^a expansions velocity of the bullets			
Region	N_e [cm^{-3}]	M/M_\odot	v [km s^{-1}]
Inner ring	500–1800	0.01–0.10	30
NE lobe	1500–3000	0.02–0.07	70 (140) ^a
SW lobe	1600–3000	0.25–0.50	70 (140) ^a

ring where it varies between 0.5:1 and 0.7:1. Only the bright knot at the southern rim of the ring has a higher ratio of 1.1:1. The $[\text{NII}]/\text{H}\alpha$ ratio is considerably larger in the bipolar lobes, with a peak value of 1.7:1 in the north-eastern lobe and around 2:1 in the south-western lobe. Thus, regions with the highest electron density also exhibit the largest $[\text{NII}]/\text{H}\alpha$ ratio.

5. Two of a Kind? – SN 1987 A and Sher 25

How does Sher 25’s circumstellar nebula compare to the inner and outer rings around SN 1987 A?

Ionization source: The progenitor of SN 1987 A had a Morgan-Keenan (MK) type of B3I (e.g., Walborn et al. 1989) and thus did not provide enough ionizing flux for the inner and outer rings to become visible before the flash ionization by the supernova explosion. Sher 25 has an MK type of B1.5I (Moffat 1983). In addition, Sher 25 is located just $20''$ (0.6 pc projected separation) north of HD 97950, the core of the young massive cluster at the center of NGC 3603. The fact that the brighter regions of the bipolar lobes are facing the cluster indicates that ionizing photons and/or fast stellar winds from the cluster’s O and WR stars (e.g., Drissen et al. 1995) provide an external ionization source. The cap at the tip of the south-western lobe faces the direction of motion (see below). Compression might be responsible for the higher flux observed here.

Morphology: High spatial resolution observations of SN 1987 A (e.g., Wampler et al. 1990; Plait et al. 1995; Panagia et al. 1996) revealed the presence of an inner ring with a diameter of 0.4 pc and two outer rings 0.4 pc above and below the plane of the inner ring (Cumming & Lundqvist 1997). The width of the inner ring appears to be $\leq 0''.12$ (0.030 pc at 50 kpc; Plait et al. 1995) and the outer rings are un-

resolved down to $0''.05$, (0.013 pc at 50 kpc; Panagia et al. 1996). While the outer rings might sit on the top and bottom of an hourglass-shaped nebula, with the inner ring around its waist, no ionized material has been detected in the interior of the hourglass. For Sher 25, the ring has a diameter of 0.4 pc and a width of 0.027 pc, and the polar lobes stretch out to 0.7 pc above and below the central plane. The complete silhouette of the hourglass can be seen in emission in the $\text{H}\alpha$ and the $[\text{NII}]$ lines.

Free electron density and mass: In the case of SN 1987 A, which lacks any external or internal ionization source besides the supernova explosion itself, only the inner ring and the two outer rings are ionized and showed peak electron densities up to 10^4 cm^{-3} shortly after the light from the supernova reached the rings (e.g., Fransson et al. 1989; Plait et al. 1995). The majority of the material within the hourglass is neutral. The mass in each ring is less than $0.008 M_\odot$ and the total mass in the hourglass amounts to $0.34 M_\odot$ to $1.7 M_\odot$ (e.g., Crots & Kunkel 1991; Burrows et al. 1995). The total ionized mass within Sher 25’s nebula is of the order of $0.3 M_\odot$ to $0.7 M_\odot$.

Kinematics: The expansion velocities of the inner ring around SN 1987 A and Sher 25 are 10 km s^{-1} and 30 km s^{-1} , respectively. The bipolar lobes recede from Sher 25 with about 70 km s^{-1} whereas the outer shell around SN 1987 A expands with a velocity of 85 km s^{-1} (Burrows et al. 1995). Based on dynamical time scales, the inner ring around SN 1987 A is about 10^4 yr younger than the outer rings, and it also shows a stronger enrichment in heavy elements (Panagia et al. 1996). The bipolar lobes and the ring around Sher 25 appear to be coeval.

$[\text{NII}]/\text{H}\alpha$ ratio: For SN 1987 A the highest $[\text{NII}]/\text{H}\alpha$ ratios were observed in the inner ring, up to 4.2:1, and smaller ratios in the outer rings, 2.5:1 (Panagia et al. 1996). Sher 25 shows an opposite behavior, the

line ratios being higher in the bipolar outflows, up to 2.1:1, than in the central ring, 1:1. Thus while the ring around Sher 25 has similar brightness in $H\alpha$ and $[NII]$, the inner ring around SN 1987A is 1.5^m brighter in $[NII]$ than in $H\alpha$.

6. Conclusion

Do the nebulae around Sher 25 and SN 1987 A belong to the same class of objects? There are many morphological similarities between the bipolar nebulae around SN 1987 A and Sher 25. We suggest that they indeed represent the first members of a new class of bipolar nebulae around blue supergiants in their final evolutionary stages. They might be situated between Luminous Blue Variables and Planetary Nebulae.

We will learn more about the structure and abundance of SN 1987 A's inner ring once the supernova remnant impinges upon the inner ring in the year 2005 ± 3 (Chevalier & Dwarkadas 1995; Pun & Kirshner 1996). In the meantime, detailed follow-up studies and theoretical modeling of the ring and hourglass nebula around Sher 25 should greatly advance our knowledge of ring structures and bipolar nebulae around blue supergiants. Compared to the rings around SN 1987 A, Sher 25 offers the advantage that it can be studied at 8 times higher spatial resolution. The hourglass structure is continuously ionized and will not rapidly fade away or be destroyed like SN 1987 A's rings. Forthcoming high spatial resolution observations of Sher 25 using the HST/WFPC2 (in Cycle 7) will enable us to study the ring structure in more detail. Understanding the formation of the nebula and analyzing its abundances will also shed light on the surface enrichment and mass loss history of the central star.

YHC acknowledges the NASA grant NAG 5-3246. EKG acknowledges support by the German Space Agency (DARA) under grant 05 OR 9103 0.

REFERENCES

Brandner, W., Grebel, E.K., Chu, Y.-H., & Weis, K. 1997, *ApJ*, 475, L45

Burrows, Ch.J., Krist, J., Hester, J.J. et al. 1995, *ApJ*, 452, 680

Chevalier, R.A. & Dwarkadas, V.V. 1995 *ApJ*, 452, L45

Clayton, C. 1986, *MNRAS*, 219, 895

Crotts, A.P.S., & Kunkel, W.E. 1991, *ApJ*, 366, L73

Cumming, R.J., Lundqvist, P. 1997 in *Advances in Stellar Evolution*, eds. R.T. Rood & A. Renzini, (CUP, Cambridge), in press

Drissen, L., Moffat, A.F.J., Walborn, N.R., & Shara, M.M. 1995, *AJ*, 110, 2235

Fransson, C., Cassatella, A., Gilmozzi, R. et al. 1989, *ApJ*, 336, 429

Moffat, A.F.J. 1983, *A&A*, 124, 273

Panagia, N., Scuderi, S., Gilmozzi, R., et al. 1996, *ApJ*, 459, L17

Plait, P.C., Lundqvist, P., Chevalier, R.A., & Kirshner, R.P. 1995, *ApJ*, 439, 730

Pun, C.S., & Kirshner, R.P. 1996, *BAAS* 189, #45.04

Walborn, N.R., Prevot, M.L., Prevot, L. et al. 1989, *A&A*, 219, 299

Wampler, E.J., Wand, L., Baade, D. et al. 1990, *ApJ*, 362, L13

This 2-column preprint was prepared with the AAS L^AT_EX macros v4.0.

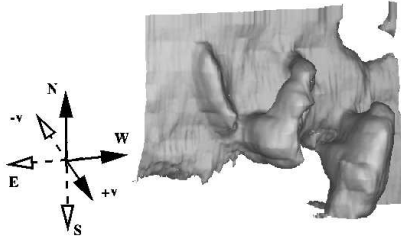
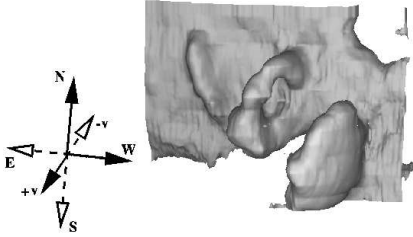
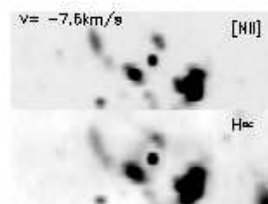
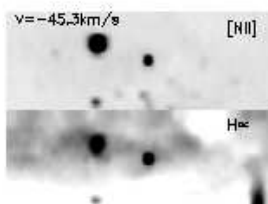
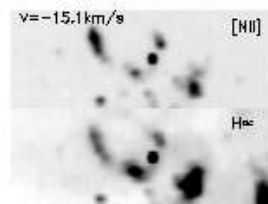
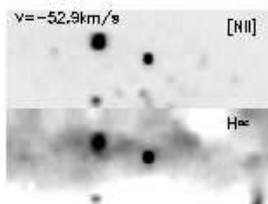
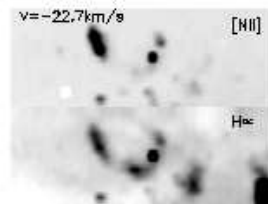
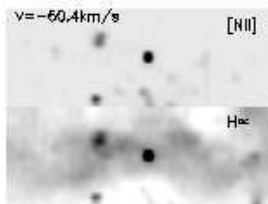
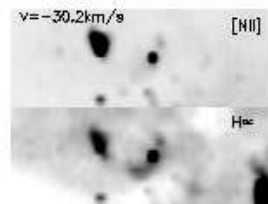
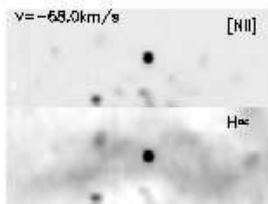
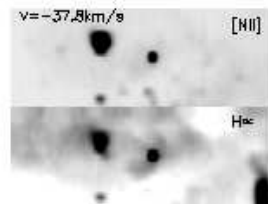
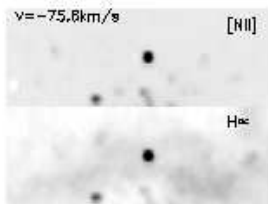


Fig. 2.— $H\alpha$ iso-surface plots of the 3-D data cube of the nebula around Sher 25 from two different viewing angles (215° , top & 165° , bottom). Note that we show the nebula as seen from ‘behind’ to prevent the redshifted portions of the nebula ($+v$) being obscured through the underlying blueshifted HII region. The field of view is $52'' \times 28''$ ($1.6\text{pc} \times 0.8\text{pc}$) and the velocity ranges from -94 km s^{-1} to $+94 \text{ km s}^{-1}$. Bright stars have been subtracted.



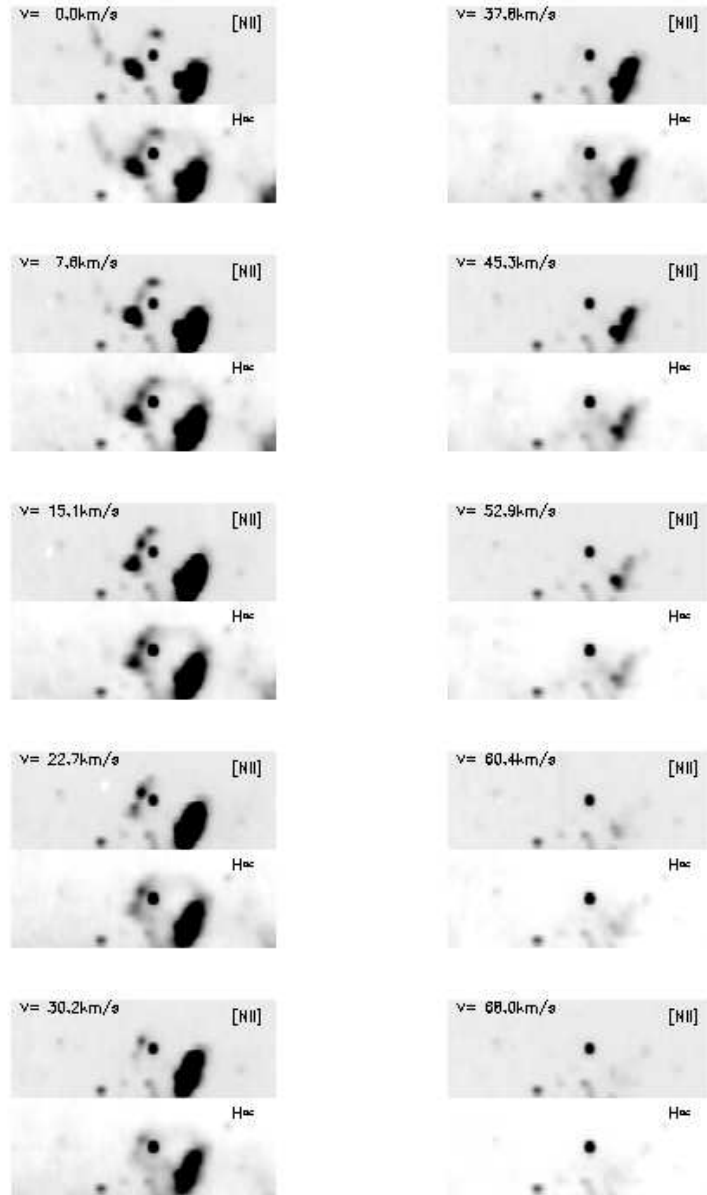


Fig. 1.— Iso-velocity maps of Sher 25’s circumstellar nebula in [NII] and H α . The field of view is $78'' \times 28''$, north is up and east is to the left.

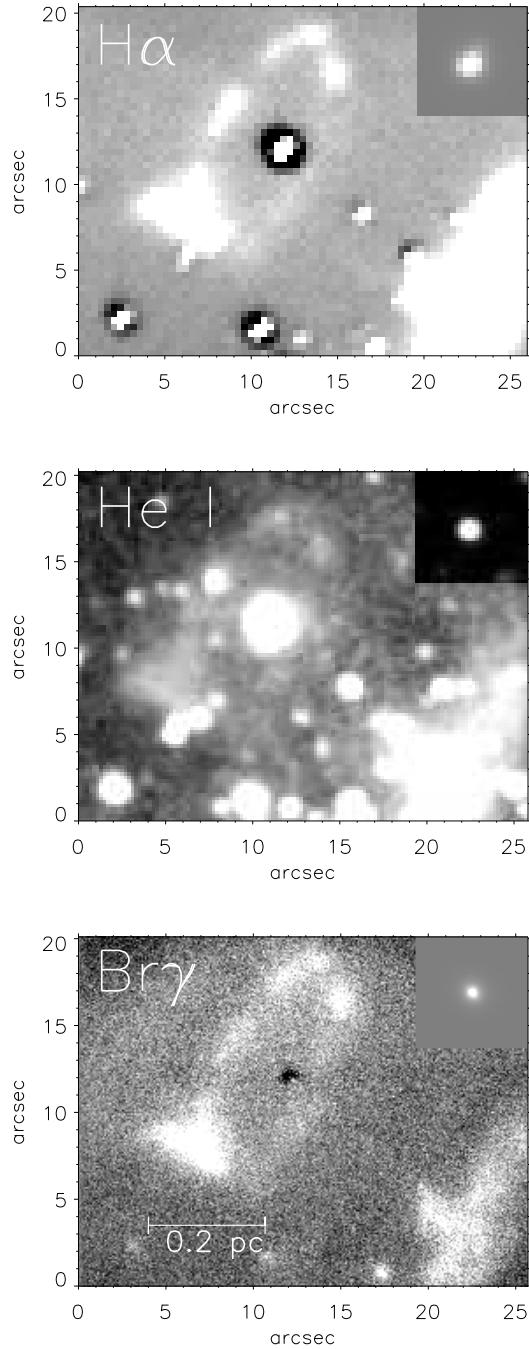


Fig. 3.— Emission-line images of Sher 25’s ring. Top: Continuum-subtracted H α image obtained with direct imaging (cf. Brandner et al. 1997). Middle: He I $1.08\ \mu\text{m}$ observations (not continuum-subtracted) obtained with HST/NICMOS (NIC3). Bottom: Continuum-subtracted Br γ image obtained with adaptive optics. The insert in the upper right corner of each panel shows the point spread function. Note that the width of the ring is clearly resolved on our near-infrared adaptive optics and HST images. A faint linear structure is visible between Sher 25 and the south-western cap. North is up and east is to the left.